J Nanopart Res (2017) 19: 306
DOI 10.1007/s11051-017-3998-0

RESEARCH PAPER

Highly selective colorimetric detection of Ni^{2+} using silver nanoparticles cofunctionalized with adenosine monophosphate and sodium dodecyl sulfonate

Jiayu Feng · Weiwei Jin · Pengcheng Huang · Fangying Wu

Received: 2 May 2017 / Accepted: 16 August 2017 / Published online: 31 August 2017

Abstract We report a dual-ligand strategy based on silver nanoparticles (AgNPs) for highly selective detection of Ni^{2+} using colorimetric techniques. Adenosine monophosphate (AMP) and sodium dodecyl sulfonate (SDS) were both used as ligands to modify AgNPs. The presence of Ni^{2+} induces the aggregation of AgNPs through cooperative electrostatic interaction and metal–ligand interaction, resulting in a color change from bright yellow to orange. The cofunctionalized AgNPs showed obvious advantages over the ones functionalized only by AMP or SDS in terms of selectivity. Under the optimized conditions, this sensing platform for Ni^{2+} works in the concentration range of 4.0 to 60 μM and has a low detection limit of 0.60 μM. In addition, the colorimetric assay is very fast, and the whole analysis can be completed within a few minutes. Thus, it can be directly used in tap water and lake water samples.

Keywords Adenosine monophosphate · Sodium dodecyl sulfonate · Colorimetry · Silver nanoparticles · Ni^{2+}

Electronic supplementary material The online version of this article (https://doi.org/10.1007/s11051-017-3998-0) contains supplementary material, which is available to authorized users.

J. Feng · W. Jin · P. Huang (✉) · F. Wu
College of Chemistry, Nanchang University, Nanchang 330031, China
e-mail: pchuang@ncu.edu.cn

Introduction

Some metal ions are crucial components of living organisms, serving as cofactors for numerous proteins with diverse functions (Yang et al. 2016). Nickel is an essential trace element to biota for its biological functions. It can form complex with amino acids, peptides, phosphates, and other biotic ligand models like nucleic acids (Ragsdale 2008), and it is a biologically important metal ion (Tedsana et al. 2015). Nickel not only stimulates certain enzymes but also plays important roles in various enzyme activities such as hydrogenases, superoxide dismutases, and catalytic processes. However, the amount of nickel we need is very little; an excess of nickel ion in either organism may be thus a toxic metal from biological point of view resulting in pneumonitis, asthma, lung cancer, and also certain disorder of the central nervous system as well as the respiratory system (Deblina et al. 2016). Hence, Ni^{2+} detection and quantification is of considerable significance (Li et al. 2009).

There are various analytical methods for detection of Ni^{2+} such as atomic absorption spectrometry (Sun et al. 2006), microwave-induced plasma atomic emission spectrometry (Jankowski et al. 2005), membrane- and potentiometric-based techniques (Gupta et al. 2007), fluorescence (Ganjali et al. 2015), electrochemistry, and chromatography (Tedsana et al. 2015). These methods are sensitive and reliable, but involve high cost, sophisticated instrumentations, and are time-consuming. Therefore, it is important to develop simple, sensitive, and selective methods for determination of trace amounts of nickel.

Nowadays, colorimetric methods, in particular, are extremely attractive because the detection results can be easily read out with the bare eyes. Moreover, they offer advantages of simplicity, rapidity, cost effectiveness, and no requirement of any sophisticated instrumentation. Gold and silver nanoparticles (AuNPs/AgNPs) have been widely adopted as colorimetric sensors to provide alternative schemes to conventional detection methods for metal ions (Kumar and Anthony 2014). AuNPs/AgNPs of various sizes and shapes can be synthesized and surface-modified with different functionalities. Furthermore, they exhibit excellent biocompatibility and unique optoelectronic and chemical properties (Pourreza et al. 2015; Yin et al. 2002; Chen et al. 2014a, b; Noh et al. 2015; Chen et al. 2014a, b). Many works related to the detection of Ni^{2+} by Au/Ag nanoparticle-based colorimetric assays have been reported. Li s group demonstrated the glutathione-modified AgNPs to detect Ni^{2+} (Li et al. 2009). Zhang s group also developed the peptide-modified AuNPs for parallel detection of Cd^{2+}, Ni^{2+}, and Co^{2+} (Zhang et al. 2012). Annadhasaan s group reported a method for Ni^{2+} and Co^{2+} based on green synthesis of AuNPs under sunlight irradiation (Annadhasan et al. 2015). The detailed comparison is organized in Table S1. As summarized, these methods' sensitivity and selectivity need to be improved. Therefore, establishing methods to detect Ni^{2+} sensitively and selectively is still demanding.

Compared to gold, silver is relatively abundant and inexpensive, and AgNPs are popular for the outstanding chemical and physical properties, such as size- and shape-depending optical, electrical, biological, and magnetic properties (Isabel et al. 2011; Pourreza et al. 2015). AgNPs are also widely used in various fields such as catalysis (Joseph and Mathew, 2015), optics (Kang et al. 2014), imaging (Tai et al. 2007), cancer therapy (Austin et al. 2014; Carolina et al. 2014), and sensor technology (Filippo et al. 2013; Rameshkumar et al. 2014). Obviously, the distance-dependent surface plasmon resonance (SPR) absorption of AgNPs have become a useful tool for the development of colorimetric sensing with various analytes. We develop a simple colorimetric nanosensor for the determination of Ni^{2+} by using the interparticle plasmon coupling on analyte-induced aggregation of AgNPs modified with two specific recognition ligands, sodium dodecyl sulfonate (SDS), and adenosine monophosphate (AMP). SDS and AMP were both commercially available, and they were bound onto the AgNPs through the sulfonic group and amino group. Owing to cooperative effect of electrostatic interaction between Ni^{2+} and SDS and coordination interaction between Ni^{2+} and AMP, well-dispersed AMP-SDS-AgNPs were readily aggregated in the presence of Ni^{2+}. And consequently, the color of AMP-SDS-AgNPs underwent dramatic change from bright yellow to orange. According to the color change, the concentrations of Ni^{2+} can be easily estimated by bare eyes without the aid of the sophisticated and expensive instruments. Scheme 1 outlines the possible sensing mechanism.

Experimental

Materials and instruments

All chemicals used were of analytical grade and were used without further purification. Silver nitrate ($AgNO_3$), sodium borohydride ($NaBH_4$), adenosine monophosphate (AMP), sodium dodecyl sulfate (SDS), NaOH, HCl, and compounds of the metallic ions ($AlCl_3$, $BaCl_2$, $CaCl_2$, $CdCl_2$, $CoCl_2$, $CrCl_3$, $Cu(NO_3)_2$, $FeCl_3$, $HgCl_2$, KCl, $MgCl_2$, $MnCl_2$, NaCl, NH_4Cl, $ZnSO_4$, $Pb(NO_3)_2$, $FeSO_4$, and $NiCl_2$) were purchased from Shanghai Qingxi Technology Co., Ltd. (Shanghai, China, www.ce-r.cn/sites/qingxi/). Milli-Q purified ultrapure water was used to prepare all the solution tested. All the glassware used must thoroughly be washed with freshly prepared aqua regia (3:1; HCl/HNO_3) and then rinsed comprehensively with ultrapure water and air-dried prior to use.

Ultraviolet-visible (UV-vis) absorption spectra were examined on a UV-2550 spectrophotometer (Shimadzu, Kyoto, Japan) using a 1.0-cm quartz cell at room temperature. Transmission electron microscope (TEM) was recorded by a JEM-2100 transmission electron microscope (JEOL Ltd. Japan, www.jeol.cn). Fourier transform infrared (FT-IR) spectra were recorded with KBr pellets on a Nicolet 5700 FT-IR Spectrometer (Nicolet, USA, www.thermonicolet.com). The data of dynamic light scattering (DLS) were obtained on NPA152 nanoparticle size analyzer (Microtrac Inc., USA, www.malvern.com/en/).

Synthesis of AMP-SDS-AgNPs

The AgNPs were prepared according to the previously reported method (Li et al. 2010) in which the $AgNO_3$

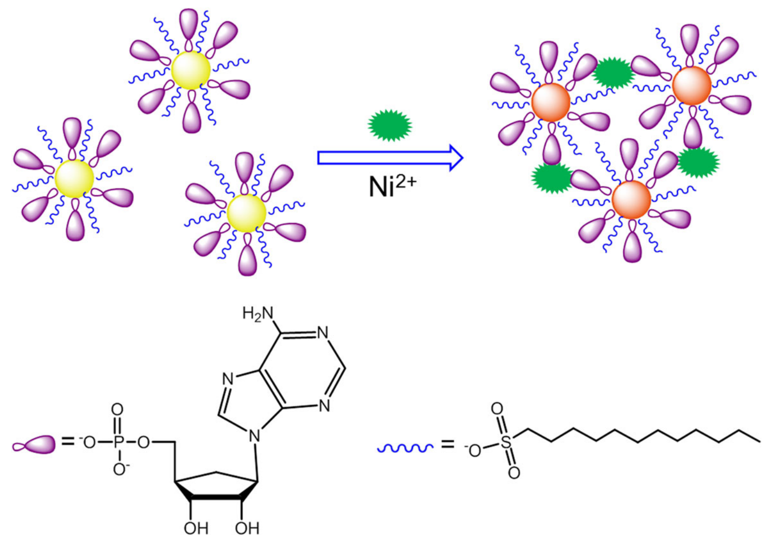

Scheme 1 Colorimetric assay of Ni^{2+} based on the aggregation mechanism using AMP-SDS-AgNPs

was reduced to Ag using $NaBH_4$. Briefly, in a flask, 2.0 mL of 0.01 M $AgNO_3$ was added into 96.8 mL doubly distilled water. Then 8.8 mg of $NaBH_4$ was quickly added into the above mixture solution under vigorous stirring for 30 min at room temperature (25 ± 2 °C); 1.0 mL of 0.01 M AMP and 0.2 mL of 0.01 M SDS were then added into the above aqueous solution. The resulting yellow silver colloidal solution was stirred for 2 h in the dark room. The resulting yellow silver colloidal solution was stored at 4 °C in the dark before use.

Colorimetric detection of Ni^{2+}

In a typical experiment, 2.0 mL of AMP-SDS-AgNPs was mixed with different Ni^{2+} concentrations in the range of 0 to 60 μM. Finally, the color changes were detected by the bare eye and by UV-vis absorption spectra. The photographs were taken with a digital camera, and the UV-vis spectra were recorded between 300 and 800 nm. The absorbance ratio at 515 and 396 nm (A_{515nm}/A_{396nm}) has been used as the index parameter of AMP-SDS-AgNPs for detection of Ni^{2+} and the numerator and the denominator represent the degree of dispersion and aggregation, respectively. All the experiments were performed in triplicate. Limit of detection (LOD) values was calculated using the following equation: LOD = 3 S_0/K, where S_0 is the standard deviation of blank measurements (n = 10) and K is the slope of calibration line.

Results and discussion

Response of AMP-SDS-AgNPs to Ni^{2+}

Figure 1a shows absorption spectral change of AMP-SDS-AgNPs upon addition of Ni^{2+}; the absorbance at 396 nm of AgNPs which was ascribed to plasmon band decreased and a new absorption band at 515 nm appeared. Meanwhile, the color changed from yellow to orange (inset of Fig. 1a). The above changes were attributed to the aggregation of AMP-SDS-AgNPs, which was also supported by TEM graph changes. Figure 1b shows the TEM image of well-dispersed NPs, and Fig. 1c presented the TEM image of NPs after the addition of Ni^{2+} where the particles were found agglomerated and the average size of the NPs was much larger than dispersed NPs. In addition, the DLS measurements were used to monitor the change in the average hydrodynamic size of AMP-SDS-AgNPs. As shown in Fig. S1, after the addition of Ni^{2+}, the size of NPs was greatly increased from 9.8 ± 3.5 to 58.3 ± 15.3 nm. The result obtained with DLS was similar to TEM measurement, also suggesting that Ni^{2+} can result in the effective aggregation of AMP-SDS-AgNPs.

Detection mechanism for Ni^{2+}

To gain insight into the interactions between various functional groups of SDS, AMP, and AgNPs, FT-IR spectra measurements were carried out. Figure S2

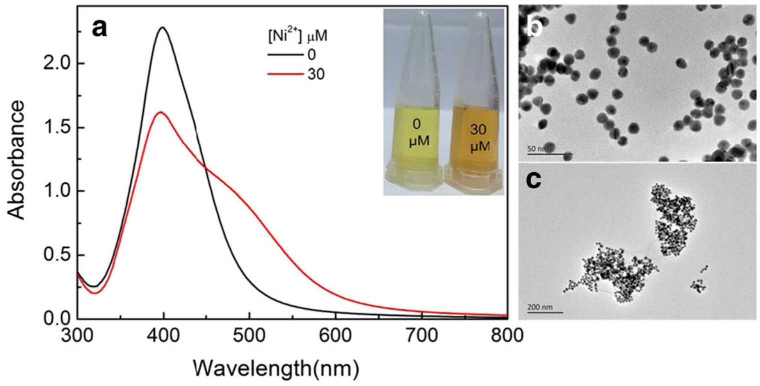

Fig. 1 **a** UV-vis spectra of AMP-SDS-AgNPs in the absence and presence of 30 μM Ni^{2+} (inset image is colorimetric response of AMP-SDS-AgNPs to Ni^{2+}), and TEM images of AMP-SDS-AgNPs in the absence (**b**) and presence (**c**) of 30 μM Ni^{2+}

compared the characteristic stretching frequencies for SDS, AMP, and AMP-SDS-AgNPs. It is noteworthy that the S=O stretching vibration band at 1260–1109 cm^{-1} of sulfonic group is obvious for SDS and disappears for AMP-SDS-AgNPs. Furthermore, the band at 900–650 cm^{-1} assigned to the characteristic peaks of C–N stretching vibrations is clearly shown in the spectrum of AMP and disappears for AMP-SDS-AgNPs. Based on the FT-IR spectra, we concluded that SDS and AMP were co-modified on the surface of AgNPs through the sulfonic group and the amino group.

Ni^{2+} is known to bind well to groups or ligands containing lone pair electron such as $-NH_2$, imidazole, etc. via the coordination bond (Deblina et al., 2016; Kang et al. 2017). Therefore, it may be the N of imidazole in the AMP on the outer surface of the AMP-SDS-AgNPs that was responsible for sensing Ni^{2+} based on metal–ligand interactions to form a stable complex. It is noted that electrostatic interaction between Ni^{2+} and SDS also play an important role, as demonstrated below. Thus, a fast and efficient interparticle cross-linking of the AgNPs occurred in the presence of Ni^{2+}.

Optimization of detection conditions

Effect of AMP concentration

Parameter ascertainment and optimization of the present method are the key factors to its performance in terms of effectiveness and sensitivity, which strongly depend on the AMP concentrations. Since SDS only acts as stabilizer, we mainly investigate the effect of the ratio of the AgNPs and AMP. Therefore, AMP at different concentrations was added to the AgNPs. As shown in Fig. S3, as the ratio of AgNPs and AMP rises, the degree of AgNPs aggregation increases, as is reflected by the ratio of absorbance values at 515 and 396 nm (A_{515nm}/A_{396nm}), while an obvious change in A_{515nm}/A_{396nm} cannot be observed when the ratio of the AgNPs and

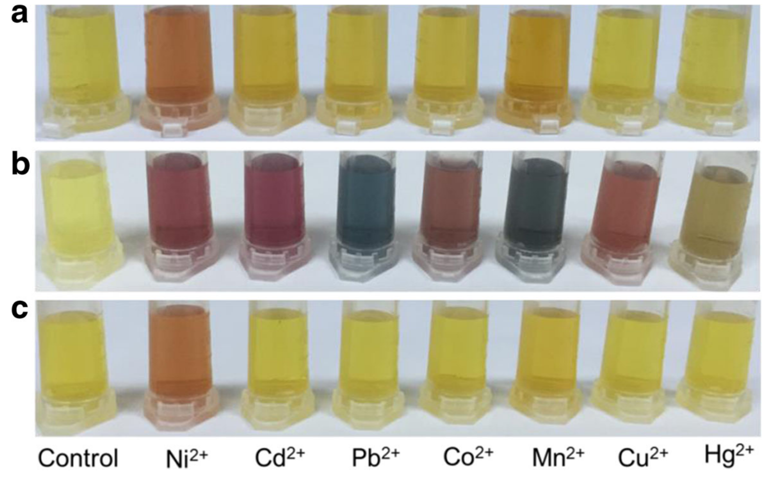

Fig. 2 **a** AMP-AgNPs, **b** SDS-AgNPs, and **c** AMP-SDS-AgNPs solution in the presence of different metal ions (30 μM)

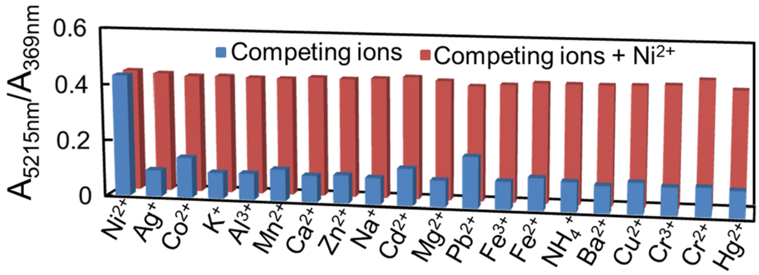

Fig. 3 Selectivity of the AMP-SDS-AgNPs for Ni^{2+}. (blue) bars represent the extinction ratio of AMP-SDS-AgNPs in the presence of Ni^{2+} or several other competing ions (30 μM), and (red) bars are the response from mixture of Ni^{2+} (30 μM) and maximum tolerant amount of competing species.

AMP was higher than 2:1. In contrast, when the molar ratio of AgNPs and AMP was lower than 2:1, both the homogeneity of the AgNPs and the capability of Ni^{2+} detection became worse. Based on these results, the ratio of the AgNPs and AMP was chosen to be 2:1 in the following experiments.

Effect of pH and reaction time

It is significant to choose optimal reaction conditions that determine enough aggregation of AgNPs, so sample pH value and reaction time were also investigated.

The aggregation of silver nanoparticles can be influenced by factors such as media pH. Therefore, the pH condition for the Ni^{2+} detection method was optimized in the range of 4.0–11.0. Media pH was adjusted using 1.0 M NaOH and 1.0 M HCl. The molar ratio (A_{515nm}/A_{396nm}) of AMP-SDS-AgNPs showed no obvious change with the pH value increasing from 4.0 to 7.0 after the addition of 30 μM Ni^{2+}. By contrast, the absorbance ratio (A_{515nm}/A_{396nm}) of AMP-SDS-AgNPs changed evidently when the pH value is more than 8.0 (Fig. S4a). The result indicated that AMP-SDS-AgNPs can be more sensitive in the presence of Ni^{2+} under alkaline environment. Since the pH value of the prepared AMP-SDS-AgNPs was 9.5, to save the time and cost, pH 9.5 which was the condition of the prepared SAA-AgNPs without any pH adjustments was selected.

To determine the interaction time required for aggregation of nanoparticles, change in absorption spectra of silver nanoparticles after addition of Ni^{2+} was observed and absorbance ratio (A_{515nm}/A_{396nm}) was plotted against time. As shown in Fig. S4b, for the three concentrations that had been examined, it is remarkable that the absorbance ratio of AMP-SDS-AgNPs increased rapidly with time once the Ni^{2+} was added to the AMP-SDS-AgNPs solution and reached a relatively constant value in 5 min, which was in good agreement with the color change observed by the bare eyes, revealing that the aggregation of AMP-

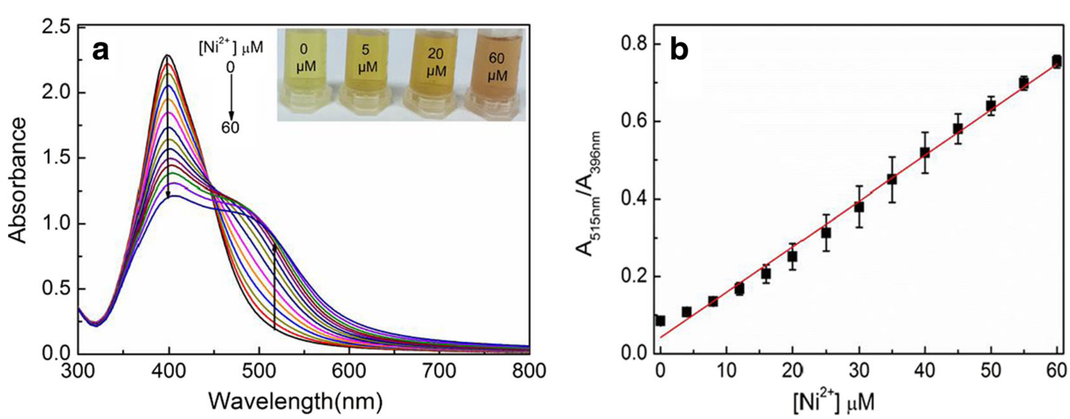

Fig. 4 **a** Absorption spectra of the AMP-SDS-AgNPs in the presence of Ni^{2+} with various concentrations at 0, 5.0, 8.0, 12, 16, 20, 25, 30, 35, 40, 45, 50, 55, and 60 μM, respectively. Inset is the corresponding photograph. **b** The plot of absorbance ratio (A_{515nm}/A_{396nm}) of AMP-SDS-AgNPs versus the concentration of Ni^{2+}

Table 1 Recovery test results of the assay in tap and lake water samples with spiked Ni^{2+}

Sample	Added (μM)	Found (μM)	Recovery (%)	RSD (%) ($n = 3$)
Tap water	0	Not found	–	–
	12	11.7 ± 0.15	97.2	1.32
	30	32.9 ± 2.65	109	8.03
	45	44.9 ± 1.61	99.7	3.59
Lake water	0	Not found	–	–
	12	12.1 ± 1.35	100	11.2
	30	32.4 ± 3.15	107	9.71
	45	47.3 ± 1.53	105	3.23

SDS-AgNPs was able to be completed within 5 min under this condition.

Selectivity of AMP-SDS-AgNPs

Specific recognition is an important criterion by which to evaluate the performance of the colorimetric sensor for Ni^{2+} detection. The effects of common existing metal ions such as Cd^{2+}, Al^{3+}, Ba^{2+}, Ca^{2+}, Cu^{2+}, Ag^{+}, Co^{2+}, Cr^{3+}, Fe^{3+}, Mg^{2+}, Hg^{2+}, K^{+}, Mn^{2+}, NH_4^{+}, Zn^{2+}, Fe^{2+}, Cr^{2+}, and Pb^{2+} were investigated, in which all the metal ions' concentration is 30 μM. Figure S5 showed the UV-vis absorption spectra and photographic images of AMP-SDS-AgNPs solution after adding various metal ions. It was found that only the presence of Ni^{2+} can induce distinct changes of AMP-SDS-AgNPs both in absorption spectrum and the color of the solution change from yellow to orange. These results indicate that the present method can be potentially used to detect Ni^{2+} in aqueous solution with high selectivity.

To further demonstrate the assay for highly selected colorimetric visualization of Ni^{2+}, we had employed AMP-AgNPs and SDS-AgNPs as control experiments. The solution of SDS-AgNPs underwent vivid color change for many metal ions (Fig. 2b), like Ni^{2+}, Cd^{2+}, Pb^{2+}, Co^{2+}, Mn^{2+}, and Cu^{2+}, which is attributed to be electrostatic interaction resulting in very poor selectivity. AMP-AgNPs showed a similar color change as those of AMP-SDS-AgNPs except for Mn^{2+} (Fig. 2a), which suggests metal ion binds with N atom of AMP. In fact, only the presence of Ni^{2+} led to the color change of AMP-SDS-AgNPs (Fig. 2c), demonstrating that AgNPs decorated with AMP and SDS exhibited excellent selectivity to Ni^{2+} over the ones functionalized only by AMP or SDS. This should mainly result from the cooperative effect of electrostatic interaction between Ni^{2+} and SDS and coordination interaction between Ni^{2+} and AMP.

Interference analysis of the assay

To determine the specificity of present colorimetric method for detection of Ni^{2+}, we investigated the possible interference of common adulterants. As showed in Fig. 3, the presence of following amounts of foreign species compared with the concentration of Ni^{2+} resulted in less than ± 10% error: 100 times the concentration of K^{+}, Na^{+}, and Al^{3+}, 60 times the concentration of Ca^{2+}, 50 times the concentration of Co^{2+}, NH_4^{+}, and Cu^{2+}, 30 times the concentration of Cd^{2+}, Mg^{2+}, Ba^{2+}, and Cr^{2+}, 10 times the concentration of Ag^{+}, Mn^{2+}, Zn^{2+}, Fe^{3+}, Fe^{2+}, Cr^{3+}, and Hg^{2+}, and 5 times the concentration of Pb^{2+}. The above results indicate good selectivity of the present colorimetric assay for Ni^{2+} over potentially interfering compounds.

Sensitivity of our assay for Ni^{2+}

Under the above optimized conditions, in order to establish AMP-SDS-AgNPs as a sensing probe, we developed analytical assay for the quantification of Ni^{2+} in aqueous solution. To this, different concentrations of Ni^{2+} were added individually into AMP-SDS-AgNPs and corresponding UV-vis absorption spectra were measured. As noticed in Fig. 4a, upon incremental addition of Ni^{2+} to AMP-SDS-AgNPs in aqueous solution, the SPR absorption peak at 396 nm decreased with the appearance of a new diffident peak at 515 nm. It was observed that by increasing the concentration of from 4.0 to 60 μM, the absorbance ratio (A_{515nm}/A_{396nm}) linearly increased as shown in Fig. 4b. This indicated that the aggregation of the AMP-SDS-AgNPs was directly related to the Ni^{2+} concentration. When the absorbance ratios (A_{515nm}/A_{396nm}) were plotted against the concentrations of Ni^{2+}, a linear correlation coefficient (R) of 0.997 (regression equation of $y = 0.012 \times + 0.414$) was obtained within the concentration range of Ni^{2+} from 4.0 to 60 μM. The limit of detection (LOD) for Ni^{2+} was 0.6 μM, which was much lower than the maximum contaminant level of Ni^{2+} (45 μM) in drinking water by the US Environmental Protection Agency (EPA).

Practical application

In order to validate the reliability of our method, lake water and tap water samples were evaluated for Ni^{2+} using the aforementioned methodology. In addition, recovery experiments using spiked real samples with three different concentrations of Ni^{2+} were performed and are summarized in Table 1. The results indicate good recoveries in the range of 98.4 to 106%. Average recovery value of 99% was obtained, indicating that the colorimetric assay can be used for the detection of Ni^{2+} in real samples from different fields with high accuracy.

Conclusions

In summary, we have developed a colorimetric probe for Ni^{2+} based on the aggregation of AMP- and SDS-cofunctionalized AgNPs. The functionalized AgNPs for colorimetric sensing of Ni^{2+} exhibited much higher selectivity over the counterparts modified only with AMP or SDS. This is attributed to be electrostatic interaction between Ni^{2+} and SDS, and Ni^{2+} binds with N atom of AMP. Thus, AMP- and SDS-functionalized AgNPs provide an effective pathway for rapid, sensitive, selective, and visual detection of Ni^{2+} in the presence of other metal ions.

Author contributions The first two authors contributed equally to this work.

Funding This study was funded by the Natural Science Foundation of China (no. 21505067).

Compliance with ethical standards

Conflict of interest The authors declare that they have no conflict of interest.

References

Annadhasan M, Kasthuri J, Rajendiran (2015) Green synthesis of gold nanoparticles under sunlight irradiation and their colorimetric detection of Ni^{2+} and Co^{2+} ions. RSC Adv 5:11458–11468

Austin LA, Mackey MA, Dreaden EC, Ei-Sayed MA (2014) The optical, photothermal, and facile surface chemical properties of gold and silver nanoparticles in biodiagnostics, therapy, and drug delivery. Arch Toxicol 88:1391–1417

Carolina Alves DS, Marcelo Martins S, Avinash PI, Indarchand G, Stefania G, Massimiliano G, Aniket G, Mahendra R (2014) Silver nanoparticles: therapeutical uses, toxicity, and safety issues. Pharm Sci 103:1931–1944

Chen GH, Chen WY, Yen YC, Wang CW, Chang HT, Chen CF (2014a) Detection of mercury(II) ions using colorimetric gold nanoparticles on paper-based analytical devices. Anal Chem 86:6843–6849

Chen L, Li JH, Chen LX (2014b) Colorimetric detection of mercury species based on functionalized gold nanoparticles. ACS Appl Mater Interfaces 6:15897–15904

Deblina S, Kumar PA, Kumar MT (2016) Benzimidazole based ratiometric and colourimetric chemosensor for Ni^{2+}. Spectrochim Acta A 153:397–401

Filippo E, Manno D, Buccolieri A, Serra A (2013) Green synthesis of sucralose-capped silver nanoparticles for fast colorimetric triethylamine detection. Sensors Actuators B Chem 178:1–9

Ganjali MR, Hosseini M, Motalebi M, Sedaghat M, Mizani F, Faridbod F, Norouzi P (2015) Selective recognition of Ni^{2+} ion based on fluorescence enhancement chemosensor. Spectrochim Acta A 140:283–287

Gupta VK, Goyal RN, Agarwal S, Kumar P, Bachheti N (2007) Nickel(II)-selective sensor based on dibenzo-18-crown-6 in PVC matrix. Talanta 71:795–800

Isabel D, Paula E, Monika O, Markus BL, Olli I, Robin HAR (2011) Functionalization of nanofibrillated cellulose with silver nanoclusters: fluorescence and antibacterial activity. Macromol Biosci 11:1185–1191

Jankowski K, Yao J, Kasiura K, Jackowska A, Sieradzka A (2005) Multielement determination of heavy metals in water samples by continuous powder introduction microwave-induced plasma atomic emission spectrometry after preconcentration on activated carbon. Spectrochim Acta B 60:369–375

Joseph S, Mathew B (2015) Microwave-assisted green synthesis of silver nanoparticles and the study on catalytic activity in the degradation of dyes. J Mol Liq 204:184–191

Kang JH, Lee SY, Ahn HM, Kim C (2017) A novel colorimetric chemosensor for the sequential detection of Ni^{2+} and CN^{-} in aqueous solution. Sensors Actuators B Chem 242:25–34

Kang Y, Wu T, Liu BX, Wang X, Du YP (2014) Selective determination of mercury (Hg^{2+}) by self-referenced surface-enhanced raman scattering using dialkyne-modified silver nanoparticles. Microchim Acta 181:1333–1339

Kumar VV, Anthony SP (2014) Silver nanoparticles based selective colorimetric sensor for Cd^{2+}, Hg^{2+} and Pb^{2+} ions: tuning sensitivity and selectivity using co-stabilizing agents. Sensors Actuators B Chem 191:31–36

Li HB, Cui ZM, Han CP (2009) Glutathione-stabilized silver nanoparticles as colorimetric sensor for Ni^{2+} ion. Sensors Actuators B Chem 143:87–92

Li HB, Li FY, Han CP, Cui ZM, Xie GY, Zhang AQ (2010) Highly sensitive and selective tryptophan colorimetric sensor based on 4,4-bipyridine-functionalized silver nanoparticles. Sensors Actuators B Chem 145:194–199

Noh KC, Nam YS, Lee HJ, Lee KB (2015) A colorimetric probe to determination Pb^{2+} using functionalized silver nanoparticles. Analyst 140:8209–8216

Pourreza N, Golmohammadi H, Naghdi T, Yousefi H (2015) Green in-situ synthesized silver nanoparticles embedded in bacterial cellulose nanopaper as a bionanocomposite plasmonic sensor. Biosens Bioelectron 74:353–359

Ragsdale SW (2008) Nickel and its surprising impact in nature. Angew Chem Int Ed 47:824–826

Rameshkumar P, Viswanathan P, Ramaraj R (2014) Silicate sol-gel stabilized silver nanoparticles for sensor applications toward mercuric ions, hydrogen peroxide and nitrobenzene. Sensors Actuators B Chem 202:1070–1077

Sun ZM, Liang P, Ding Q, Cao J (2006) Determination of trace nickel in water samples by cloud point extraction preconcentration coupled with graphite furnace atomic absorption spectrometry. J Hazard Mater 137:943–946

Tai SP, Wu Y, Shieh DB, Chen LJ, Lin KJ, Yu CH, Chu SW, Chang CH, Shi XY, Wen YC (2007) Molecular imaging of cancer cells using plasmon-resonant-enhanced third-harmonic-generation in silver nanoparticles. Adv Mater 19: 4520–4523

Tedsana W, Tuntulani T, Ngeontae W (2015) A circular dichroism sensor for Ni^{2+} and Co^{2+} based on L-cysteine capped cadmium sulfide quantum dots. Anal Chim Acta 867:1–8

Yang Y, Yuan Z, Liu XP, Liu Q, Mao CJ, Niu HL, Jin BK, Zhang SY (2016) Electrochemical biosensor for Ni^{2+} detection based on a DNAzyme-CdSe nanocomposite. Biosens Bioelectron 77:13–18

Yin YD, Li ZY, Zhong ZY, Gates B, Xia YN, Venkateswaran S (2002) Synthesis and characterization of stable aqueous dispersions of silver nanoparticles through the Tollens process. J Mater Chem 12:522–527

Zhang M, Liu YQ, Ye BC (2012) Colorimetric assay for parallel detection of Cd^{2+}, Ni^{2+} and Co^{2+} using peptide-modified gold nanoparticles. Analyst 137:601–607